Flow, Turbulence and Combustion (2024) 112:1191–1213
https://doi.org/10.1007/s10494-024-00537-3

RESEARCH

On the Definition of Reaction Progress Variable in Exhaust Gas Recirculation Type Turbulent MILD Combustion of Methane and n-Heptane

Khalil Abo-Amsha[1] · Hazem S. A. M. Awad[1] · Umair Ahmed[1] · Nilanjan Chakraborty[1] · Nedunchezhian Swaminathan[2]

Received: 19 September 2023 / Accepted: 19 February 2024 / Published online: 22 March 2024

Abstract
Three-dimensional Direct Numerical Simulations of Exhaust Gas Recirculation (EGR)-type Moderate or Intense Low Oxygen Dilution (MILD) combustion of homogeneous mixtures of methane- and n-heptane–air have been conducted with skeletal chemical mechanisms. The suitability of different choices of reaction progress variable (which is supposed to increase monotonically from zero in the unburned gas to one in fully burned products) based on the mass fractions of different major species and non-dimensional temperature have been analysed in detail. It has been found that reaction progress variable definitions based on oxygen mass fraction, and linear combination of CO, CO_2, H_2 and H_2O mass fractions (i.e. c_{O2} and c_c) capture all the extreme values of the major species in the range between zero and one under MILD conditions. A reaction progress variable based on fuel mass fraction is found to be unsuitable for heavy hydrocarbons, such as n-heptane, since the fuel breaks down to smaller molecules before the major reactants (products) are completely consumed (formed). Moreover, it has been found that the reaction rates of c_{O2} and c_c exhibit approximate linear behaviours with the heat release rate in both methane and n-heptane MILD combustion. The interdependence of different mass fractions in the EGR-type homogeneous mixture combustion is considerably different from the corresponding 1D unstretched premixed flames. The current findings indicate that the tabulated chemistry approach based on premixed laminar flames may need to be modified to account for EGR-type MILD combustion. Furthermore, both the reaction rate and scalar dissipation rate of c_{O2} and c_c are found to be non-linearly related in both methane and n-heptane MILD combustion cases but the qualitative nature of this correlation for n-heptane is different from that in methane. This suggests that the range of validity of SDR-based turbulent combustion models can be different for homogeneous MILD combustion of different fuels.

Keywords MILD combustion · Exhaust Gas Recirculation · Reaction progress variable · Heat release rate · Scalar dissipation rate

✉ Nilanjan Chakraborty
nilanjan.chakraborty@ncl.ac.uk

[1] School of Engineering, Newcastle University, Newcastle upon Tyne NE1 7RU, UK

[2] Cambridge University Engineering Department, Trumpington Street, Cambridge CB2 1PZ, UK

1 Introduction

Moderate or Intense Low Oxygen Dilution (MILD) combustion has been identified as one of the promising technologies for ensuring high energy efficiency and low emissions (Cavaliere and de Joannon 2004). In MILD combustion, the reactants are preheated above their autoignition temperature (Cavaliere and de Joannon 2004), and this preheating is often obtained by recirculating the hot flue gas back into the combustion chamber (Tsuji et al. 2003). Moreover, the maximum temperature rise in MILD combustion also remains smaller than the self-ignition temperature of the reacting mixture (Cavaliere and de Joannon 2004; Tsuji et al. 2003). MILD combustion offers advantages in terms of providing a uniform temperature distribution, extremely low NOx and CO emissions and high thermal efficiency. All these advantageous features make MILD combustion an attractive proposition for gas turbines and process applications (Cavaliere and de Joannon 2004; Tsuji et al. 2003). However, the oxygen concentration in gas turbine combustion is often much greater than the values required for MILD combustion and thus a large amount of exhaust gas needs to be recirculated to obtain an optimum ultra-lean, diluted, and preheated mixture. This acts to reduce energy density and temperature rise, which adversely affect the thrust-weight/power-weight ratio of gas turbine combustors. Moreover, high velocity and low O_2 concentration make the ignition and flame stabilisation difficult and under these conditions, blowout and flame quenching become highly likely for aero- and land-based gas turbines (Duwig et al. 2008). These challenges currently prohibit MILD combustion from being used widely in gas turbines, and in most cases, applications of MILD combustion are found in process-heating sectors. Thus, an improved fundamental understanding of MILD combustion is urgently needed to take advantage of this promising methodology at a time when the necessity of high efficiency and low emission has never been greater (Duwig et al. 2008).

To date, several experimental (Cavaliere and de Joannon 2004; Tsuji et al. 2003; Duwig et al. 2008, 2012; Suzukawa et al. 1997; Dally et al. 2002, 2004; Plessing et al. 1998; Özdemir and Peters 2001; Christo and Dally 2005; Medwell et al. 2007; Oldenhof et al. 2011) and numerical (Coelho and Peters 2001; Aminian et al. 2011; van Oijen 2013; Minamoto et al. 2013, 2014; Minamoto and Swaminathan 2014a, b, 2015; Doan et al. 2018; Swaminathan 2019; Awad et al. 2021; Abo-Amsha and Chakraborty 2023) investigations focussed on the physics of MILD combustion, and the advancements in high-performance computing has enabled Direct Numerical Simulations (DNS) of MILD combustion (van Oijen 2013; Minamoto et al. 2013, 2014; Minamoto and Swaminathan 2014a, b, 2015; Doan et al. 2018; Swaminathan 2019; Awad et al. 2021; Abo-Amsha and Chakraborty 2023). These analyses provide valuable insights into the physics of the MILD combustion process and help to explain the differences between MILD combustion and the conventional combustion processes in terms of reaction zone thickness and its morphology (Minamoto et al. 2013, 2014; Minamoto and Swaminathan 2014a, b, 2015; Doan et al. 2018; Swaminathan 2019; Awad et al. 2021; Abo-Amsha and Chakraborty 2023). However, most of the analyses of MILD combustion were conducted for simple fuels such as H_2 (van Oijen 2013), CH_4 (Duwig et al. 2008, 2012; Suzukawa et al. 1997; Dally et al. 2002, 2004; Plessing et al. 1998; Özdemir and Peters 2001; Christo and Dally 2005; Medwell et al. 2007; Minamoto et al. 2013, 2014; Minamoto and Swaminathan 2014a, b, 2015; Doan et al. 2018; Swaminathan 2019; Awad et al. 2021), C_2H_4 (Dally et al. 2004) and C_3H_8 (Dally et al. 2004) while limited attention is given to the MILD combustion of heavier hydrocarbons (e.g. C_7H_{16}) (Ye et al. 2017; Abo-Amsha and Chakraborty 2023), which are

often used in industrial furnaces and gas turbines. Therefore, it is useful to compare the MILD combustion processes for simple fuels such as CH_4 and a heavy hydrocarbon such as n-heptane C_7H_{16} (as it is often used in industrial applications) to assess whether the physical insights gained and the resulting models developed based on MILD combustion of CH_4 are applicable for heavier hydrocarbons (e.g. n-heptane). In this respect, it is worthwhile to consider the choice of reaction progress variable that can be used in the parameterisation of MILD combustion of these two fuels, and thus allows for the identification of a methodology applicable to MILD combustion of different fuels (Duwig et al. 2007; Ihme and See 2012; Chen et al. 2017; Göktolga et al. 2017; Romero-Anton et al. 2020; Huang et al. 2022). It is worth noting that a single reaction progress variable may not be sufficient to fully characterise the MILD combustion process since it is not able to capture fuel cracking, radical pool build-up and pollutant formation. However, the reaction progress variable can play a useful role in modelling the overall progress of the chemical conversion in the context of RANS and LES of MILD combustion (Duwig et al. 2007; Ihme and See 2011; Chen et al. 2017; Göktolga et al. 2017; Romero-Anton et al. 2020; Huang et al. 2022). In fact, the reaction progress variable is used commonly as one of the input parameters for the tabulated chemistry (Duwig et al. 2007; Göktolga et al. 2017; Romero-Anton et al. 2020; Huang et al. 2022) and presumed PDF (Ihme and See 2011; Chen et al. 2017) approaches employed for MILD combustion. Moreover, this approach was used in several studies on premixed and partially premixed combustion (Proch et al. 2017). This aspect is particularly important because it is not straightforward to define a reaction progress variable in a multispecies system (Papapostolou et al. 2019; Keil et al. 2021), but identification of a suitable reaction progress variable is necessary from the point of view of generating flamelet and tabulated chemistry-based closures for conventional and MILD combustion processes (de Swart et al. 2010; Ihme and See 2011; Aminian et al.2012; Lamouroux et al. 2014; Abtahizadeh et al. 2015; De and Dongre 2015; Langella et al. 2016; Sorrentino et al. 2017).

Many different automated approaches for defining the reaction progress variable have been reported in the literature (Ihme et al. 2012; Najafi-Yazdi et al. 2012; Niu et al. 2013; Prüfert et al. 2015; Vasavan et al. 2020; Rahnama et al. 2023). However, since the analysis of the choice of reaction progress variable definition in MILD combustion has not reached the same level of maturity as that in the case of conventional combustion, it is useful to consider the behaviour of the normalised species variations in MILD combustion. Such analysis can be considered as a first step in the identification of species subsets that form plausible input variables to an automated method for the optimal definition of reaction progress variables in MILD combustion, and provides the knowledge required to judge the output of such automated methodologies. In this context, the current study only considers definitions of the reaction progress variable based on individual major species and an example of species combination that has been used in the literature, while the investigation of automated methodologies for the definition of reaction progress variable is kept beyond the scope of the current work. By investigating different definitions of the reaction progress variable, this study aims to analyse the sensitivity of MILD combustion characteristics to typical progress variable definitions.

The present analysis considers DNS data of Exhaust Gas Recirculation (EGR)-type turbulent MILD combustion of methane and n-heptane under comparable conditions in terms of turbulence intensity, its integral length scale, and O_2 concentration. The simulation configuration is based on that used by Minamoto and co-workers (Minamoto et al. 2013, 2014; Minamoto and Swaminathan 2014a, b, 2015) for the EGR-type MILD combustion of homogeneous mixtures involving methane as the fuel.

The objectives of this study are: (1) to compare the interrelation between reaction progress variable and non-dimensional temperature in turbulent MILD combustion of methane and n-heptane; (2) to compare the interrelation between heat release rate (HRR), and the reaction rate of reaction progress variable along with their dependence on scalar dissipation rate (SDR) of reaction progress variable in the above MILD combustion cases.

2 Mathematical Background

In MILD combustion of homogeneous mixtures, the extent of completion of the chemical reaction can be characterised with the help of a reaction progress variable, which is expected to increase monotonically from zero in the unburned gases to one in fully burned products. The reaction progress variable can be defined in terms of a major species mass fraction Y_α as:

$$c_\alpha = (Y_\alpha - Y_{\alpha,u})/(Y_{\alpha,b} - Y_{\alpha,u}) \tag{1}$$

where the subscripts u and b refer to the values in the unburned and fully burned gases in the corresponding laminar premixed flames respectively. Several previous studies (Ihme and See 2011; Göktolga et al. 2017; Romero-Anton et al. 2020) considered linear combinations of species such as CO, CO_2, and H_2O to define the reaction progress variable. One such choice is (Ihme and See 2011):

$$c_c = (Y_c - Y_{c,u})/(Y_{c,b} - Y_{c,u}) \tag{2}$$

where $Y_c = Y_{CO_2} + Y_{CO} + Y_{H_2} + Y_{H_2O}$. In this study, the behaviour of c_c is also analysed. The reaction rate of c_α (as well as c_c) is given as:

$$\dot{\omega}_c = \dot{\omega}_\alpha/(Y_{\alpha,b} - Y_{\alpha,u}) \tag{3}$$

where $\dot{\omega}_\alpha$ is the reaction rate of the species, or the species combination, upon which the reaction progress variable is defined.

The progress of chemical processes can also be characterised in terms of the non-dimensional temperature $\Theta = (T - T_u)/(T_b - T_u)$ where T_u, T_b and T are the unburned gas temperature, burned gas temperature and instantaneous dimensional temperature, respectively. The source term associated with Θ is the normalised heat release rate defined as:

$$\dot{\omega}_\Theta = -\sum_{k=1}^{N} h^0_{f,k}\dot{\omega}_k/(h_{s,b} - h_{s,u}) \tag{4}$$

where $h_{s,u}$ and $h_{s,b}$ refer to the sensible enthalpies of the unburned gas and fully burned gas, respectively, and $h^0_{f,k}$ is the enthalpy of the formation of species k. Under low Mach number, adiabatic conditions, c_α becomes identical to Θ for unity Lewis number (i.e. ratio of thermal diffusivity to mass diffusivity) assumption. However, C_7H_{16} has a high Lewis number (=3.0) compared to methane (=0.97). Thus, the non-unity Lewis number effects are expected to be stronger in n-heptane than in methane combustion. Moreover, the differences in the oxidation pathways also contribute to the differences in MILD combustion of methane and n-heptane.

3 Numerical Implementation

A well-known DNS code SENGA+ (Cant 2012) is used for the simulations. In SENGA+, all the spatial derivatives are evaluated using a high-order finite-difference scheme (10th-order centred scheme for the interior nodes with the order of accuracy gradually reducing to 4th order one-sided scheme at non-periodic boundaries). For methane-air combustion, a skeletal chemical mechanism involving 16 species and 25 chemical reactions (involving 10 equilibrium reactions) (Smooke and Giovangigli 1991) has been considered. A reduced chemical mechanism involving 22 species and 18 reactions (Liu et al. 2004) is used for the n-heptane MILD simulations. The species diffusion is modelled using a constant Lewis number approach with each species having its own Lewis number value, which helps to capture differential diffusion effects. The constant Lewis numbers approach has been compared with more detailed diffusion models (i.e. the mixture-averaged and multi-component diffusion models) for calculating ignition delay time under MILD conditions and no significant differences were observed (van Oijen 2013).

The time-advancement of the governing equations (except for the chemical source term in the n-heptane simulation) has been carried out using an explicit 4th-order Runge–Kutta method. For n-heptane, due to the stiffness of the chemical mechanism (Liu et al. 2004), the species mass fractions equations have been solved using the fractional step method where the linear system of ODEs in the second step (which includes the chemical source term) was solved using a variable-coefficient solver with preconditioned Krylov iteration as implemented in the VODPK package (Byrne 1992). In the methane case, the chemical source term was dealt with explicitly. In the current simulations, the boundaries in the x -direction are taken to be inlet and outlet, while the boundaries in the y- and z-directions are periodic.

For the methane-air MILD combustion case, the unburned gas temperature is taken to be 1500 K for CH_4-oxidiser mixtures with an O_2 mole fraction of 4.8% and an equivalence ratio of $\phi = 0.8$. This leads to an unstretched laminar burning velocity S_L of 3.20m/s. It is worth noting that, at temperatures above the mixture's autoignition temperature, the laminar burning velocity S_L value is not unique and depends on the domain size (Minamoto et al. 2014). Thus, when calculating the values of S_L in this study, the domain length of the 1D unstretched laminar flame simulation was chosen to be similar to that of the DNS domain. Moreover, the values of S_L and the thermal flame thickness ($\delta_{th} = (T_b - T_u)/\max|\nabla T|_L$ with the subscript L referring to the unstretched laminar flame quantities) are reported here only to help identify the parametric range of the current analysis.

A mean inlet velocity $U_{inlet} = 30$m/s is used for the methane MILD case where the root-mean-square (rms) turbulent velocity u'_{inlet} and integral length scale ℓ at the inlet are taken to be $12.48\text{m/s} = 4.0S_L$ and $1.7\text{mm} \approx 2.0\delta_{th}$, respectively. These conditions are representative of the experimental analysis by Suzukawa et al. (1997). For the n-heptane case, the unburned reactant temperature is taken to be 1100K and the fuel-oxidiser mixture has an O_2 mole fraction of 4.5% for an equivalence ratio of $\phi = 0.8$, which is consistent with the experiments by Ye et al. (2017). These conditions yield an unstretched laminar burning velocity S_L of 0.42m/s under atmospheric pressure. For n-heptane MILD combustion simulation $U_{inlet} = 6.0$m/s, $u'_{inlet} = 2.0$ m/s $= 4.76S_L$ and $\ell = 2.0\text{mm} = 1.25\delta_{th}$ are considered. These flow parameters are comparable to the experimental conditions reported by Oldenhof et al. (2011). The simulation parameters including u'/S_L, ℓ/δ_{th}, u'_{inlet}/U_{mean}, $Da = \ell S_L/u'_{inlet}\delta_{th}$ and $Ka = \left(u'_{inlet}/S_L\right)^{3/2}\left(\ell/\delta_{th}\right)^{-1/2}$ are listed in Table 1. These conditions represent relatively similar values of turbulence intensity u'_{inlet}/S_L and integral length scale of turbulence ℓ/δ_{th}.

Table 1 Simulation parameters for methane and n-heptane cases

Case	u'_{inlet}/S_L	ℓ/δ_{th}	u'_{inlet}/U_{mean}	Da	Ka	η(m)
Methane	4.0	2.08	0.42	0.52	5.54	7.7×10^{-5}
n-heptane	4.76	1.25	0.33	0.26	9.28	1.6×10^{-4}

While a direct comparison with the exact same parameters for both methane and n-heptane is not feasible due to the very different chemical scales associated with the combustion of those two fuels, the parameters used in the current study are close enough to yield a meaningful comparison. Furthermore, it is worth noting that a direct quantitative comparison is not made in the following discussion between methane and n-heptane MILD combustion cases and thus the differences in simulation parameters will not influence any of the conclusions drawn in this paper.

The simulation domain is taken to be a cube of side $L_{domain} = 10$mm and 20 mm for the methane and n-heptane MILD combustion cases, respectively. These domain sizes are comparable in terms of thermal flame thickness δ_{th} (i.e. domain length is equal to $14.5\delta_{th}$ and $12.5\delta_{th}$ for methane and n-heptane cases, respectively). The thicker flame for the n-heptane case necessitates a larger domain length than in the methane case for comparable values of L_{domain}/δ_{th}. The computational domain is discretised by a uniform Cartesian grid of $252 \times 252 \times 252$ and $216 \times 216 \times 216$ for methane and n-heptane cases, respectively which ensures about 15 grid points within δ_{th} of the respective cases.

The computational grid ensures that the reaction zone thickness $\delta_r = \delta_{th}/\beta$ (with β being the Zel'dovich number $\beta = T_{ac}(T_{ad} - T_u)/T_{ad}^2$ and T_{ac} is the activation temperature based on the theoretical solution for premixed flame) is resolved using about 5 grid points for the cases considered here. It is worth noting that this resolution is estimated based on the steepest gradient of temperature so in reality, more grid points reside within the reaction zone (Poinsot and Veynante 2001). The Kolmogorov length scale is estimated as $\eta = \ell^{0.25}(\nu)^{0.75}/u'^{0.75}$ (with u' and ℓ being the rms velocity fluctuation and integral length scale evaluated over the whole domain, and ν being the kinematic viscosity) and assumes a value of $7.7 \times 10^{-5}m$ and $1.6 \times 10^{-4}m$ for the methane and n-heptane cases, respectively (see Table 1).

The numerical procedure used in the current analysis is based on that developed by Minamoto and co-workers (Minamoto et al. 2013, 2014; Minamoto and Swaminathan 2014a, 2015) and involves the following steps:

1. The generation of a homogenous isotropic field using a pseudo-spectral method of Rogallo (1981) for the initialisation of turbulent velocity fluctuations.
2. Simulations of one-dimensional unstretched freely propagating laminar premixed flames corresponding to the thermochemical conditions summarised in Table 2 have been conducted. The solutions of these simulations (species mass fractions) were then parameterised as functions of the reaction progress variable based on O_2 (i.e. $Y_{\alpha,L} = \mathcal{F}_\alpha(c_{O2,L})$).

Table 2 Thermochemical conditions

Fuel	X_{O_2}	X_{CO_2}	X_{H_2O}	X_{fuel}	ϕ	T_u(K)
Methane	4.8%	6.1%	12.1%	1.9%	0.8	1500
n-heptane	4.5%	9.7%	11.2%	0.33%	0.8	1100

3. To provide the initial scalar field based on the corresponding laminar flame solution, a bimodal distribution of c based on O_2 mass fraction with a scalar integral length scale of $\ell_c = 1.20\ell$ is created using the methodology developed by Eswaran and Pope (1988). This bimodal distribution of c in the initial condition allows one to have a field containing unburnt, burnt and reacting mixtures based on the corresponding laminar flame solution. The initial bimodal distribution retains the variations of the scalar (in this case the reaction progress variable variation) for a longer period. Any other distribution such as Gaussian yields most of the samples around the prescribed mean leading to quicker homogenisation of the scalar field.
4. The functions developed in step 2 are then used to populate the bimodal distribution of c from the previous step, and thus initialising the density and scalar fields (species mass fractions) with atmospheric pressure and an unburned gas temperature of $T_u = 1500$ K (1100 K) for methane (n-heptane) case.
5. The initialised scalar fields in the previous step are then allowed to evolve with turbulence without reaction for about one eddy turnover time (ℓ/u') in a periodic domain mimicking the mixing process in an EGR-type MILD combustor. The temperature in the pre-processed mixture has a variation of about $\pm$0.3% of its mean value. It is worth noting that, for the considered mixture compositions (see Table 2) at the corresponding T_u, the ignition delay time is much larger than the eddy turnover time resulting from the turbulence levels considered in this study. This remains the case despite the sizable radical pool present in the initial field, since it was shown that the existence of radicals in the reactant mixture has a limited impact on the ignition delay time in MILD combustion (Sidey et al. 2014). Thus, allowing the initial scalar field to develop with turbulence does not affect the combustion process.

The evolution of the scalar fields and turbulence in step 5 acts as an auxiliary simulation that provides a mixture (containing unburnt, partially burnt, and fully burnt pockets) similar to that produced under EGR conditions. The prepared scalar field at the end of the auxiliary simulation (i.e. step 5) is then fed into the DNS domain at the inflow boundary, with a mean velocity U_{inlet}, by scanning a plane through it as used previously by Minamoto and co-workers (Minamoto et al. 2013, 2014; Minamoto and Swaminathan 2014a, b, 2015). Interested readers are referred to Awad et al. (2021) and Abo-Amsha and Chakraborty (2023) for further information regarding the CH_4 and C_7H_{16} DNS cases, respectively.

The simulations have been conducted for 2.5 pass-through times (i.e. $2.5L_{domain}/U_{inlet}$) for both methane and n-heptane cases and statistics have been extracted after 1.0 through-pass time by which the initial transience has decayed. The simulation time corresponds to 11.0 and 8.33 initial eddy turnover times, respectively. The same analysis has been conducted at 1.5 through-pass time to check for transient effects, but the same trends were returned which indicate that the analysis pursued in this paper is not time-dependent.

4 Results and Discussion

The distributions of non-dimensional temperature Θ for methane and n-heptane cases are shown in Figs. 1a and b, respectively. Figures 1a and b show that in both cases Θ changes in a continuous manner instead of a sharp gradient between zero (representing unburned gas temperature) and one (representing burned gas temperature), as obtained in

conventional premixed flames. This is consistent with experimental observations (Plessing et al. 1998; Özdemir and Peters 2001) and previous DNS (Minamoto et al. 2013, 2014; Minamoto and Swaminathan 2014a, 2015) results. The instantaneous views of the $c_{O2} = c^*$ isosurface (where c^* is the value of c_{O2} corresponding to the maximum heat release rate in the unstretched laminar premixed flame, which is 0.6 and 0.71 for methane and n-heptane cases, respectively) are shown in Figs. 1c and d for methane and n-heptane cases, respectively. A significant amount of self-interaction of flame elements can be seen in both cases from Figs. 1c and d, which is consistent with previous experimental (Plessing et al. 1998; Özdemir and Peters 2001; Dally et al. 2004; Christo and Dally 2005; Medwell et al. 2007; Duwig et al. 2012; Oldenhof et al. 2011) and computational (Minamoto et al. 2013, 2014; Minamoto and Swaminathan 2014a, 2015) observations. These interactions lead to the appearance of the thickened (or distributed) reaction zones, which are qualitatively similar for both cases considered here.

4.1 Evaluation of Reaction Progress Variable Definition

The mean values of non-dimensional temperature Θ, and reaction progress variables based on fuel mass fraction, and the mass fractions of major species such as CO_2 and H_2O conditional upon c_{O2}, for turbulent MILD methane and n-heptane combustion cases are shown in

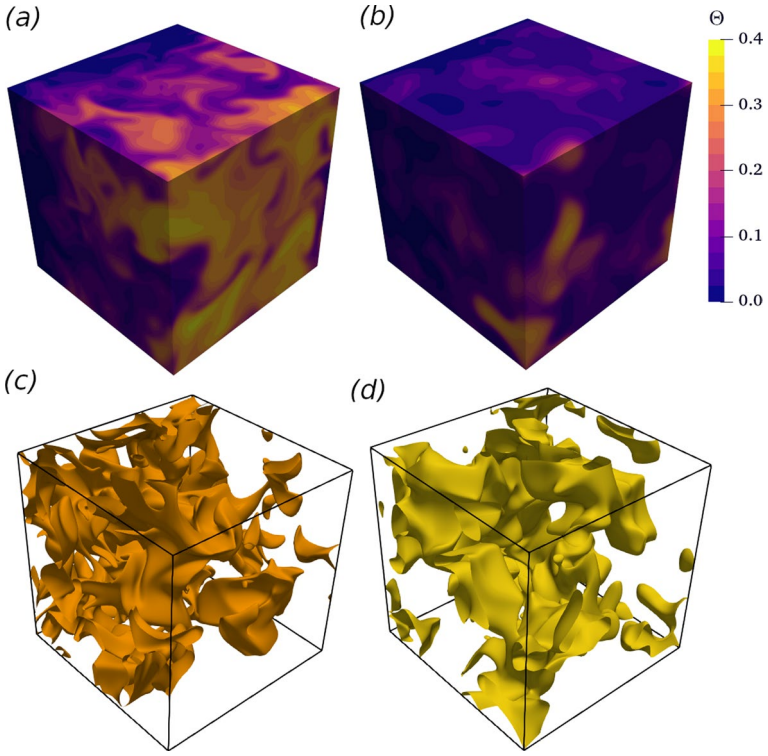

Fig. 1 Instantaneous views of Θ (**a, b**) and c_{O2} (**c, d**) isosurfaces corresponding to the maximum heat release rate for the corresponding 1D laminar premixed flame for the composition listed in Table 2 for CH_4 (**a, c**) and C_7H_{16} (**b, d**) cases

Figs. 2a and b, respectively, along with the corresponding variations for the unstretched 1D laminar flame simulations with compositions listed in Table 2. The choice of 1D diluted laminar premixed flames as a basis for comparison was made in keeping with the procedure used by Minamoto and Swaminathan (2014a). This does not constitute an endorsement of laminar premixed flames as a suitable, or even workable, base configuration for tabulation approaches. In fact, when compared to the progress variable profiles in 0D homogeneous constant pressure reactor, the 1D simulations produce qualitatively similar behaviour for the progress variables based on major species. The profiles of the reaction progress variables (based on fuel, CO_2 and H_2O) and non-dimensional temperature as functions of c_{O2} calculated from both the 0D and 1D configurations with the initial states in Table 2 are shown in Appendix A. A more in-depth comparison between the progress variable behaviour in 0D homogeneous reactors and 1D diluted premixed flames remains beyond the scope of the present analysis and will not be discussed any further. Moreover, since several previous analyses on MILD combustion (Duwig et al. 2007; Göktolga et al. 2017; Romero-Anton et al. 2020; Huang et al. 2022) have used tabulated chemistry approaches based on

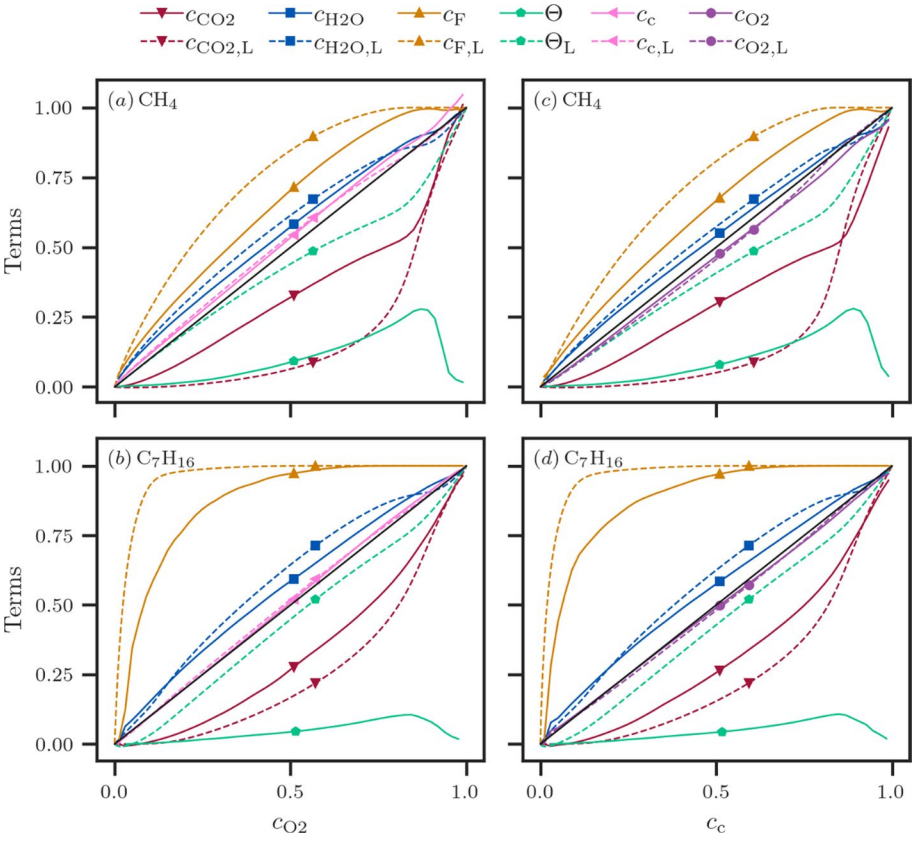

Fig. 2 Profiles of mean values of $c_F, c_{CO2}, c_{H2O}, c_c$ and Θ conditional upon c_{O2} for CH_4 (**a**) and C_7H_{16} (**b**) cases. Profiles of mean values of $c_F, c_{O2}, c_{CO2}, c_{H2O}$ and Θ conditional upon c_c for CH_4 (**c**) and C_7H_{16} (**d**) cases. The conditions for the corresponding 1D unstretched laminar premixed flames are listed in Table 2 and shown by broken lines

laminar premixed flame solutions, the following discussion will principally focus on the comparison of turbulent flow simulation results with the corresponding findings from 1D unstretched laminar flame solutions.

Figures 2a and b show that c_F, c_{CO2}, c_{H2O}, and Θ are non-linearly related to c_{O2} in turbulent MILD combustion cases for both methane and n-heptane. This non-linear dependence also exists for the corresponding unstretched 1D laminar flame simulations. The preferential diffusion due to non-unity Lewis number (i.e. $Le \neq 1.0$) along with the differences in spatial distributions of these species arising from different chemical conversion rates give rise to this non-linearity, which is further augmented under turbulent conditions since the effects of preferential diffusion strengthen in the presence of curvature due to local focussing/defocussing of species with $Le \neq 1.0$. Although the presence of species with non-unity Lewis number can lead to local effects of preferential diffusion, the global effect of preferential diffusion is not strong to yield super-/sub-adiabatic values of major species mass fractions in both cases considered here. This is also valid for conventional premixed flames and a recent investigation by Keil et al. (2021) and Awad et al. (2022) for methane-air premixed flames demonstrated considerable local preferential diffusion effects but reaction progress variable and non-dimensional temperature does not exhibit super-/sub-adiabatic values. Similarly, all the different choices of reaction progress variable remain bound between zero and one for both CH_4 and C_7H_{16} MILD combustion cases considered here.

A comparison between Figs. 2a and b reveals that the non-linearity between the scalar quantities presented in these figures is stronger in the n-heptane case than in the methane case. This is particularly evident in the profiles of c_F variation with c_{O2}. Figures 2a and b show that the mean value of c_F attains 1.0 for a much smaller value of c_{O2} in the n-heptane case compared to that in the methane case. In the case of n-heptane, at high temperatures, C_7H_{16} readily breaks down to smaller intermediate hydrocarbon species, whereas this behaviour is not predominant in the methane case. Moreover, the Lewis numbers of CH_4 and O_2 are close to unity (i.e. 0.97 and 1.10, respectively) and therefore, the variation of mean values of c_F conditional upon c_{O2} does not depart significantly from a linear variation.

On the other hand, C_7H_{16} has a Lewis number significantly greater than unity (i.e. 3.0) which also contributes to the strongly non-linear variation of c_F with c_{O2} in this case. In both methane and n-heptane MILD combustion cases, the variations of mean values of c_{CO2} conditional upon c_{O2} exhibit non-linear behaviours and a similar qualitative behaviour has been observed for the corresponding 1D unstretched laminar premixed flames. The Lewis number of CO_2 is 1.39 in contrast to a Lewis number of 1.10 for O_2, which contributes to the non-linear interrelation between c_{CO2} and c_{O2}. Although the Lewis number of H_2O remains close to unity ($=0.83$), the variation of the mean value of c_{H2O} conditional on c_{O2} exhibits a mildly non-monotonic behaviour for both methane and n-heptane turbulent MILD combustion cases and qualitatively similar behaviour is observed for the corresponding 1D laminar unstretched laminar flame solution. This behaviour originates from the non-monotonic variation of H_2O within the reaction zone, which has been demonstrated in a recent analysis for CH_4-air premixed flames (Keil et al. 2021).

It is important to note that highlighting the linear/non-linear behaviour of a reaction progress variable in the above discussion is merely descriptive of the profiles shown in Fig. 2 and not meant to diminish the fact that a unique mapping of scalars onto the progress variable can be achieved with either linear or non-linear progress variable behaviour as long as the behaviour is monotonic. This unique mapping of scalars to a progress variable is the essential criteria required for tabulated chemistry approaches, while linear mapping is just a desirable feature.

Figures 2a and b show that the mean values of Θ conditioned upon c_{O2} for both methane and n-heptane turbulent MILD cases, behave significantly differently to the corresponding variation obtained from the 1D unstretched laminar premixed flames corresponding to the compositions listed in Table 2. The peak mean value of Θ conditioned upon c_{O2} remains significantly smaller than unity suggesting that the temperature rise in the case of MILD combustion is smaller than in the case of the corresponding 1D premixed flame. The variations of the mean values of Θ conditioned upon c_{O2} for both methane and n-heptane MILD combustion exhibit qualitatively similar non-monotonic trends which show a drop in the mean temperature conditioned on c_{O2} from a peak value as c_{O2} approaches unity (i.e. $c_{O2} \rightarrow 1.0$). It remains infeasible to categorically isolate a single reason for the behaviour of the non-dimensional temperature (Θ) in the turbulent cases. In the present configuration, the initial mixture for the turbulent cases is made up of reactants and products of the laminar premixed flame corresponding to X_{O2} reported in Table 2. This initial mixture is designed to have a constant temperature (T_u) and a bimodal distribution of c_{O2} with peaks at $c_{O2} \approx 0$ and $c_{O2} \approx 1.0$. Therefore, the mean oxygen concentration in the turbulent MILD cases is appreciably smaller than that in the corresponding 1D unstretched laminar premixed flames. The reduced levels of average O_2 concentration in the turbulent cases due to the initialisation procedure constitute a clear discrepancy between the laminar and turbulent cases and may help in justifying the overall reduction in temperature levels in the turbulent cases since, on average, the combustion process in these cases will be more starved of oxygen than in the laminar ones. Moreover, a careful observation of Fig. 2 reveals that the drop in the mean value of Θ occurs when $c_F \approx 1.0$ but while c_{CO2} continues to rise. This suggests that the drop in the mean values of Θ conditioned upon c_{O2} at $c_{O2} \gtrsim 0.9$ occurs in a region with a combination of high average concentration of combustion products (which increases the mixture's specific heat), a reduced mean O_2 concentration and almost absent fuel species. The reduced levels of fuel and O_2 yield a rapid decrease in the heat release rate (as can be seen later from Fig. 3). The reduction in heat release rate at $c_{O2} \gtrsim 0.9$ (or $c_c \gtrsim 0.9$), along with increasing mixture specific heat due to elevated concentration of product species such as CO_2, act to reduce the temperature rise in the region where $c_{O2} \gtrsim 0.9$. The local distribution of Θ in the turbulent cases in the region $c_{O2} \gtrsim 0.9$ ($c_c \gtrsim 0.9$) can be appreciated from the scatter of Θ with c_{O2} and c_c, which are shown in Appendix B for further elucidation of the aforementioned discussion. Here, it is worth noting that, while the average O_2 concentration in the turbulent case is appreciably lower than that in the laminar case, locally there exists pockets within the 3D turbulent field that have an identical composition to that of the laminar case reactants. In fact, a wide range of mixture compositions are present within the 3D turbulent initial fields. This range spans from the composition of the laminar flames' reactants to their products. Thus, the behaviour seen in the laminar cases can be accurately reflected within local subsections of the turbulent case, but not on average.

The observations made from Fig. 2 suggest that a reaction progress variable based on fuel mass fraction may not be appropriate for the analysis of turbulent MILD combustion of heavy hydrocarbons such as n-heptane, as the chemical reactions continue to occur, and the temperature continues to rise even after c_F attains a value of unity. This is consistent with the findings of numerous previous studies concerned with modelling of long-chain hydrocarbons. The non-monotonic variation of H_2O within the reaction zone also raises uncertainty about the appropriateness of the usage of c_{H2O} as a reliable reaction progress variable. The preferential diffusion induced by the non-unity Lewis number of CO_2 may also induce complexities in parameterising other quantities in terms of reaction progress variable because the strength of preferential diffusion may alter depending on turbulence

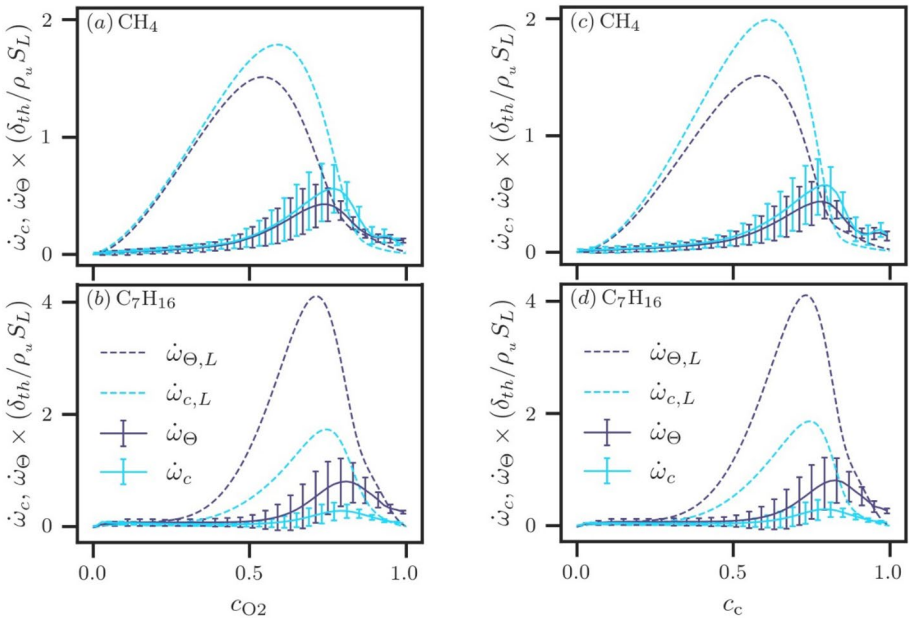

Fig. 3 Profiles of $\dot{\omega}_\Theta \times \delta_{th}/\rho_u S_L$ and $\dot{\omega}_c \times \delta_{th}/\rho_u S_L$ conditional upon c_{O2} in the CH_4 (**a**) and C_7H_{16} (**b**) cases. The same plots for c_c in the CH_4 (**c**) and C_7H_{16} (**d**) cases. The corresponding variations from 1D unstretched laminar premixed flames for the conditions listed in Table 2 are shown by broken lines in Figs. 3, 4, 5, 6. The bars indicate standard deviation values conditional upon the reaction progress variable in Figs. 3, 5, 6

level. The drop of Θ for high values of c_{O2} is not akin to conventional homogeneous mixture combustion, which also raises questions regarding the usefulness of Θ as a reaction progress variable. Moreover, Fig. 2 indicates that considering the non-dimensional temperature, in addition to the reaction progress variable, may be necessary for accurately describing MILD combustion, even for homogeneous mixtures.

The variation of the mean values of c_c conditioned on c_{O2} for both cases are also shown in Figs. 2a and b along with the corresponding variations of c_c for the laminar flames listed in Table 2. It can be seen from Figs. 2a and b that the variations of c_c with c_{O2} for both laminar and turbulent conditions remain close to each other, with c_c and c_{O2} being almost linearly related. This suggests that the profiles of mean values of c_F, c_{CO2}, c_{H2O}, and Θ conditional upon c_c are expected to be similar to the profiles of these quantities conditioned on c_{O2}. This is substantiated by Figs. 2c and d where the profiles of mean values of $c_F, c_{O2}, c_{CO2}, c_{H2O}$, and Θ conditioned on c_c are shown. A comparison between Fig. 2a, b and c, d confirms that the variations of mean values c_F, c_{CO2}, c_{H2O} and Θ conditional upon c_c are indeed similar to the corresponding variations conditional upon c_{O2} for both methane and n-heptane cases.

The findings from Fig. 2 suggest that c_{O2} and c_c can capture the extreme values of all the major species within the range given by $0.0 \leq c_{O2} \leq 1.0$ and $0.0 \leq c_c \leq 1.0$. It is worth noting that O_2 does not cause significant preferential diffusion effects as it has a Lewis number close to unity (=1.10). On the other hand, a reaction progress variable definition based on a combination of species, such as c_c, brings additional complexities in specifying the reaction progress variable diffusivity. The treatment of the reaction progress variable

diffusivity for a reaction progress variable based on a linear combination of different species mass fractions is not a straightforward task and might be strongly dependent on the choice of transport mechanism (de Swart et al. 2010; Abtahizadeh et al. 2015). While this may not be an insurmountable obstacle, it does add to the complexity of the modelling procedure. It is also worth noting that while a single progress variable will not be able to capture fuel cracking, radical pool build-up and pollutant formation, both c_{O2} and c_c are shown to be related to CO, CO_2 and H_2O formations.

The choice of reaction progress variable plays an important part in the laminar premixed flame-based tabulated chemistry approaches (e.g. de Swart et al. 2010; Lamouroux et al. 2014; Abtahizadeh et al. 2015). However, the observations made from Fig. 2 suggest that the reaction progress variable definition needs to be judiciously chosen and preferential diffusion effects due to non-unity Lewis number must be considered to extend the tabulated chemistry approaches based on laminar premixed flames for MILD combustion. Furthermore, the variations of c_F, c_{CO2}, c_{H2O}, and Θ in turbulent MILD combustion are significantly different to those in the 1D laminar premixed flame simulations with diluted mixtures corresponding to Table 2.

It is worth noting that an alternative 1D diluted laminar premixed flame simulations can be constructed by using the mean (i.e. volume averaged) values of species mass fractions after the passive scalar mixing stage of initialisation as the reactants' mixture instead of the compositions given in Table 2. This approach was used in the analyses of Minamoto et al. (2014). However, when using these alternative 1D diluted premixed flames in the current analysis, the qualitative nature of the variations of c_F, c_{CO2}, c_{H2O}, and Θ is found to be similar to those for the 1D premixed flame simulation results shown in Figs. 2a–d. Thus, these results are not explicitly shown here for the sake of conciseness.

Based on the information obtained from Fig. 2, it is useful to analyse the interrelation between the reaction rate $\dot{\omega}_c$ with the normalised heat release rate $\dot{\omega}_\Theta$ to fully assess the potential of c_{O2} and c_c as reaction progress variables to be used in the parametrisation of the reacting state under MILD conditions.

4.2 The Behaviour of Reaction Rate and Normalised HRR

The profiles of the mean values as well as the standard deviation of $\dot{\omega}_c$ and $\dot{\omega}_\Theta$ conditional upon c_{O2} for methane and n-heptane turbulent MILD cases are shown in Figs. 3a and b, respectively, along with the corresponding variations from the 1D unstretched premixed flames with the compositions listed in Table 2. Figures 3a and b show that both $\dot{\omega}_c$ and $\dot{\omega}_\Theta$ have positive mean values throughout the flame but their peak mean values for turbulent MILD combustion cases remain smaller and occur at larger c_{O2} values compared to the peak values in the corresponding 1D unstretched premixed flames. The reduced peak levels of $\dot{\omega}_c$ and $\dot{\omega}_\Theta$ is a consequence of the conditions discussed previously when explaining the reduced temperature rise under MILD conditions. When comparing the behaviour of $\dot{\omega}_c$ and $\dot{\omega}_\Theta$ in methane and n-heptane combustion, Figs. 3a and b suggest that the distributions of $\dot{\omega}_c$ and $\dot{\omega}_\Theta$ are qualitatively similar and the extent of reduction of their magnitudes under turbulent MILD conditions in comparison to that in the corresponding 1D laminar premixed flames is also comparable. However, the standard deviations of $\dot{\omega}_c$ are found to be smaller than that of $\dot{\omega}_\Theta$ in the n-heptane case, but they are comparable in the methane case. The plots corresponding to Figs. 3a and b for c_c are shown in Figs. 3c and d, respectively. A comparison between Figs. 3a, b and c, d reveals that the variations of $\dot{\omega}_c$ and $\dot{\omega}_\Theta$ with c_c remain qualitatively similar to those observed for c_{O2}.

It is worth noting that $\dot{\omega}_\Theta$ depends on the reaction rates of different species and therefore it is worthwhile to assess the correlation between the local values of $\dot{\omega}_c$ and $\dot{\omega}_\Theta$ to determine if the reaction rate of the reaction progress variable can be related to the heat release rate under MILD conditions. Figure 4 shows the mean values of $\dot{\omega}_\Theta/\left[\dot{\omega}_\Theta\right]_{L,\max}$ conditioned on $\dot{\omega}_c/\left[\dot{\omega}_c\right]_{L,\max}$ (where the subscript $L, \max$ refers to the maximum value in the 1D unstretched laminar premixed flames corresponding to the conditions summarised in Table 2) for both c_{O2} and c_c. The scatters of $\dot{\omega}_\Theta/\left[\dot{\omega}_\Theta\right]_{L,\max}$ with $\dot{\omega}_c/\left[\dot{\omega}_c\right]_{L,\max}$ are also shown in Fig. 4. It can be seen from Fig. 4 that a strong positive correlation exists between $\dot{\omega}_\Theta/\left[\dot{\omega}_\Theta\right]_{L,\max}$ and $\dot{\omega}_c/\left[\dot{\omega}_c\right]_{L,\max}$ under turbulent MILD conditions for both methane and n-heptane cases, but with qualitative differences in the scatter spread for the two fuels. This discrepancy in scatter patterns could be due to the different reaction paths contributing to the heat release rate in these two fuels. The positive correlation between $\dot{\omega}_\Theta/\left[\dot{\omega}_\Theta\right]_{L,\max}$ and $\dot{\omega}_c/\left[\dot{\omega}_c\right]_{L,\max}$ suggests that the normalised heat release rate can be expressed in terms of the reaction rate of a suitably chosen reaction progress variable in EGR-type MILD combustion.

However, Fig. 4 indicates that a predominance of finding $\dot{\omega}_\Theta/\left[\dot{\omega}_\Theta\right]_{L,\max} > \dot{\omega}_c/\left[\dot{\omega}_c\right]_{L,\max}$ is observed for the n-heptane MILD case, whereas the opposite trend is observed for the methane MILD case. This discrepancy could be due to the differences in chemical processes and preferential diffusion effects between methane and n-heptane. Figures 4c and d show that similar trends are observed for the correlation between $\dot{\omega}_\Theta/\left[\dot{\omega}_\Theta\right]_{L,\max}$ and $\dot{\omega}_c/\left[\dot{\omega}_c\right]_{L,\max}$ based on c_c compared to those for $\dot{\omega}_c/\left[\dot{\omega}_c\right]_{L,\max}$ based on c_{O2}. However,

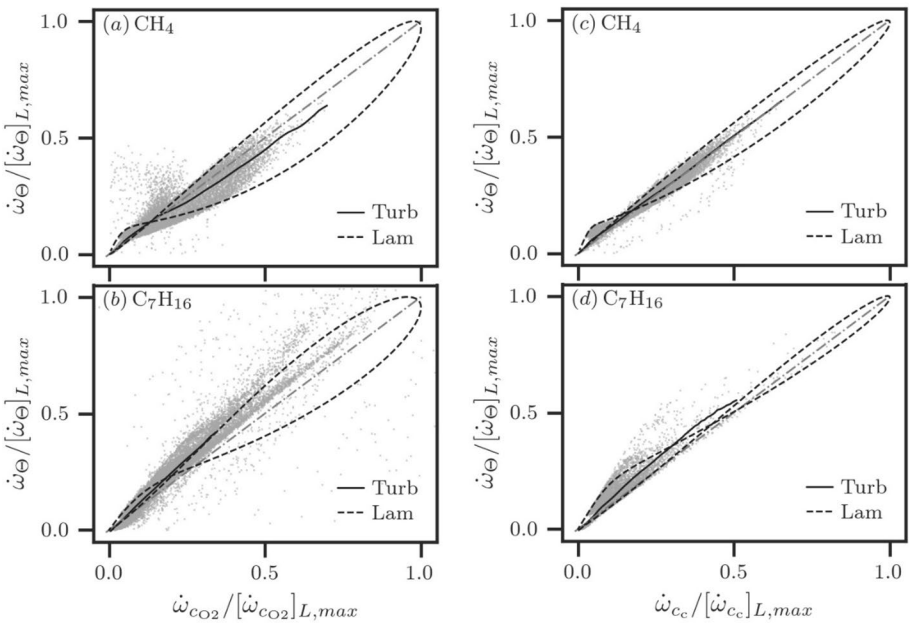

Fig. 4 Variations of the mean values, along with the scatter (in the background), of $\dot{\omega}_\Theta/\left[\dot{\omega}_\Theta\right]_{L,\max}$ conditioned upon $\dot{\omega}_c/\left[\dot{\omega}_c\right]_{L,\max}$ based on c_{O2} in the CH_4 (**a**) and C_7H_{16} (**b**) cases. The same plots for $\dot{\omega}_c/\left[\dot{\omega}_c\right]_{L,\max}$ based on c_c in the CH_4 (**c**) and C_7H_{16} (**d**) cases. Here $\dot{\omega}_\Theta/\left[\dot{\omega}_\Theta\right]_{L,\max} = \dot{\omega}_c/\left[\dot{\omega}_c\right]_{L,\max}$ are shown by the dotted-dashed line

comparing Figs. 4a, b with Figs. 4c, d reveals that the scatter for $\dot{\omega}_c/\left[\dot{\omega}_c\right]_{L,\max}$ based on c_c is smaller compared to that when $\dot{\omega}_c/\left[\dot{\omega}_c\right]_{L,\max}$ is based on c_{O2}. This indicates that using c_c as the reaction progress variable may yield a better correlation between $\dot{\omega}_\Theta/\left[\dot{\omega}_\Theta\right]_{L,\max}$ and $\dot{\omega}_c/\left[\dot{\omega}_c\right]_{L,\max}$. Figure 4 also shows that the correlations between $\dot{\omega}_\Theta/\left[\dot{\omega}_\Theta\right]_{L,\max}$ and $\dot{\omega}_c/\left[\dot{\omega}_c\right]_{L,\max}$ in the diluted laminar premixed flames exhibit multiple values of $\dot{\omega}_\Theta$ for a given $\dot{\omega}_c$. This is purely due to the shape of the $\dot{\omega}_\Theta$ and $\dot{\omega}_c$ profiles as shown in Fig. 3.

4.3 The Behaviour of the Scalar Dissipation Rate (SDR)

In the modelling of turbulent homogeneous mixture combustion, the mean/filtered reaction rate of the reaction progress variable $\overline{\dot{\omega}_c}$ (where the overbar suggests a Reynolds averaging/LES filtering operation, as appropriate) is taken to be proportional to Favre-averaged/filtered SDR $\overline{\rho}\widetilde{N}_c = \overline{\rho D_\alpha \nabla c \cdot \nabla c}$ [50] where D_α is the diffusivity of the species based on which the reaction progress variable is defined. However, these relations were originally proposed and validated using conventional premixed flames (Bray 1980; Chakraborty et al. 2011). Therefore, it is necessary to assess the mean behaviour of N_c as well as the correlation between $\dot{\omega}_c$ and N_c. The assessment of the $\dot{\omega}_c$ and N_c correlation (as opposed to $\widetilde{N}_c$) remains meaningful since the density ρ does not change appreciably under MILD conditions due to the small change in temperature.

The mean values of N_c conditional upon c_{O2} are shown in Fig. 5a, which reveals qualitatively similar behaviours for methane and n-heptane cases. The peak mean value of the SDR under MILD conditions remains considerably smaller than the peak value obtained in 1D unstretched premixed flames for the conditions listed in Table 2. The same qualitative behaviour of N_c has been observed when the corresponding variation is considered for c_c as can be seen in Fig. 5b. The diffusivity of c_c for the purpose of the evaluation of its SDR has been calculated based on a characteristic Lewis number given by $Le_c = \sum_{i=1}^{N-1} x_i' Le_i$ where $\sum_{i=1}^{N-1} x_i' = 1$ with x_i' are renormalized mole fractions for all species but excluding N_2 (which does not participate in the reaction) and Le_i is the Lewis number of individual species (Dinkelacker et al. 2011). The reduction in the mean $N_c \times \delta_{th}/S_L$ levels are a consequence of the

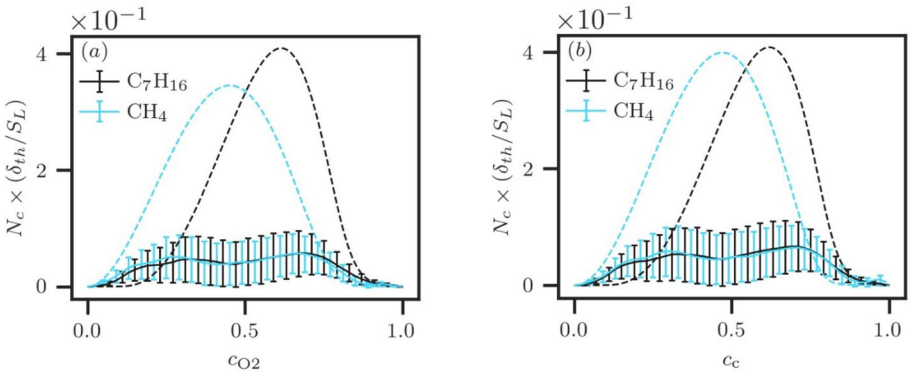

Fig. 5 Profiles of $N_c \times \delta_{th}/S_L$ conditional upon reaction progress variable for CH_4 and C_7H_{16} cases for c_{O2} (**a**) and c_c (**b**)

reduced levels of $|\nabla c|$ under turbulent MILD conditions. Recent studies (Awad et al. 2021; Abo-Amsha and Chakraborty 2023) offered explanations for the reduction of $|\nabla c|$ under turbulent conditions in both methane and n-heptane MILD combustion and interested readers are referred to Awad et al. (2021) and Abo-Amsha and Chakraborty (2023) for further information in this regard. The standard deviations of normalised SDR (i.e. $N_c \times \delta_{th}/S_L$) conditioned on c_{O2} or c_c are also shown in Fig. 5, which shows the variations around the mean value of SDR remain comparable for both cases considered here.

As already highlighted, it is useful to consider the correlations of both $\dot{\omega}_\Theta$ and $\dot{\omega}_c$ with N_c for both c_{O2} and c_c since SDR is often used for the closure of the reaction rate and heat release rate for conventional homogeneous mixture combustion (Bray 1980; Chakraborty et al. 2011). The mean and standard deviations of $\dot{\omega}_c$ conditioned on N_c within the range $0.01 \leq c_{O2} \leq 0.99$ are shown in Figs. 6a and b for the methane and n-heptane cases, respectively. The corresponding variations for c_c from both cases are shown in Figs. 6c and d, respectively.

In the methane case, both $\dot{\omega}_\Theta$ and $\dot{\omega}_c$ exhibit non-linear N_c dependence with positive and negative correlation branches, whereas both $\dot{\omega}_\Theta$ and $\dot{\omega}_c$ remain mostly positively correlated with N_c for n-heptane despite a non-linear dependence. Figure 6 shows that the standard deviations of $\dot{\omega}_\Theta \times \delta_{th}/(\rho_u S_L)$ and $\dot{\omega}_c \times \delta_{th}/(\rho_u S_L)$ has comparable levels in all cases. This non-linear N_c dependences of $\dot{\omega}_\Theta$ and $\dot{\omega}_c$ reveals that turbulent combustion modelling using SDR based on the flamelet assumption (Bray 1980; Chakraborty et al. 2011), which translates to a proportional relation between $\dot{\omega}_c$ and N_c may not be valid under MILD condition. This is consistent with previous findings for turbulent MILD combustion of methane (Minamoto et al. 2014; Minamoto and Swaminathan 2015). Moreover, Fig. 6 suggests that the dependence between $\dot{\omega}_c$ and N_c in the n-heptane case is different to that in the methane

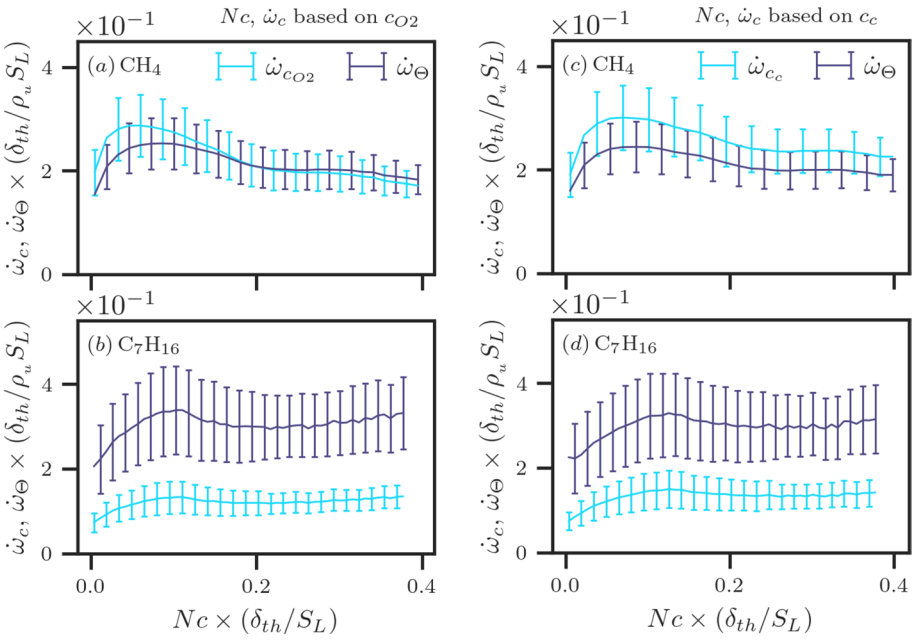

Fig. 6 Variations of the mean values of $\dot{\omega}_c \times \delta_{th}/\rho_u S_L$ and $\dot{\omega}_\Theta \times \delta_{th}/\rho_u S_L$ conditional upon $N_c \times \delta_{th}/S_L$ for c_{O2} in the range $0.01 \leq c_{O2} \leq 0.99$ for CH_4 (**a**) and C_7H_{16} (**b**) cases. The corresponding plots for c_c in the range $0.01 \leq c_c \leq 0.99$ for CH_4 (**c**) and C_7H_{16} (**d**) cases

case, which can be attributed to the differences in chemical pathway and/or differential diffusion effects and needs further investigation in future studies.

It is worth noting that MILD combustion has its distinctive features while sharing some commonality with classical modes, as has been demonstrated by Minamoto and Swaminathan (2014b) and Awad et al. (2021). It was demonstrated by Awad et al. (2021) that the strain rate and curvature dependences of displacement speed in MILD combustion are much weaker than those in conventional premixed flames. The strain and curvature effects are typically important for Flame Surface Density (FSD) based approaches, which are shown to be unsuitable for MILD combustion by Minamoto and Swaminathan (2014b) and Awad et al. (2023) and perfectly stirred reactor-based model is more appropriate (Minamoto and Swaminathan 2014b; Awad et al. 2023). The strain and curvature dependence of flame propagation does not play a major role in the modelling of MILD combustion and thus it is not explored further in the current analysis.

The findings from Figs. 2, 3, 4, 5, 6 indicate that the variations of the key quantities such as $\dot{\omega}_c$, $\dot{\omega}_\Theta$ and N_c with reaction progress variable definitions given by c_{O2} and c_c are qualitatively similar and c_{O2} and c_c are well correlated. This suggests that a reaction progress variable definition based only on O_2 mass fraction can offer comparable performance to a reaction progress variable based on a linear combination of different species mass fractions (e.g. CO, CO_2, H_2 and H_2O) (Ihme and See 2011; Göktolga et al. 2017; Romero-Anton et al. 2020). Moreover, the Lewis number of O_2 remains close to unity and the specification of diffusivity of c_{O2} is straightforward compared to c_c. Thus, the reaction progress variable transport equation can be solved in RANS/LES in the context of tabulated chemistry (de Swart et al. 2010; Ihme and See 2011; Aminian et al.2012; Lamouroux et al. 2014; Abtahizadeh et al. 2015; De and Dongre 2015; Langella et al. 2016; Sorrentino et al. 2017) approach with less uncertainty for a formulation based on c_{O2}. This corresponds to the findings of Hadadpour et al. (2023) who reported that, for spray combustion, a reaction progress variable based on oxygen performs reasonably well without requiring ad-hoc modifications. Finally, the investigation of automated methodologies for the definition of reaction progress variable (Ihme et al. 2012; Najafi-Yazdi et al. 2012; Niu et al. 2013; Prüfert et al. 2015; Vasavan et al. 2020; Rahnama et al. 2023) is kept beyond the scope of the current work. However, the current analysis provides information on the normalised species mass fraction behaviours in homogeneous mixture MILD combustion, which can be useful for future investigations in terms of automated methodologies for the definition of reaction progress variable for MILD combustion processes.

It needs to be recognised that the reaction progress variable is one of the several possible variables which are needed to parameterise a MILD combustion process. The results shown in Fig. 2 indicate that the non-dimensional temperature Θ needs to be considered in addition to the reaction progress variable for the purpose of MILD combustion parameterisation even for homogeneous (i.e. constant equivalence ratio) mixtures. Moreover, a reaction progress variable based on temperature may not adequately represent the reaction state of the combustion process under MILD conditions. Furthermore, the scatter of the key quantities such as $\dot{\omega}_c$, $\dot{\omega}_\Theta$ and N_c around their mean values conditioned upon reaction progress variable suggests that MILD combustion of homogeneous mixtures requires more than a single reaction progress variable to parameterise it. Further independent variables might be needed for parameterisation for inhomogeneous mixtures (i.e., variable equivalence ratio), which is beyond the scope of the current analysis.

5 Conclusions

Three-dimensional DNS of EGR-type MILD combustion of homogeneous mixtures for methane and n-heptane, as fuels, have been conducted using skeletal chemical mechanisms. It has been found that a fuel mass fraction-based reaction progress variable c_F may not be appropriate for heavy hydrocarbons, such as n-heptane, as it attains a value of unity before other major reactants (products) are fully consumed (formed). The preferential diffusion of CO_2 due to its Lewis number being significantly different from unity induces a significant non-linear variation of the CO_2 mass fraction-based reaction progress variable with the reaction progress variables defined based on O_2 mass fraction and a linear combination of species. A reaction progress variable based solely on H_2O mass fraction may give rise to additional uncertainties in terms of parameterising the reacting state because of its non-monotonic variation within the reaction zone. However, this does not mean that including H_2O in a combination of species upon which a rection progress variable is defined would certainly lead to a non-monotonic behaviour, as seen from the behaviour of c_c. This analysis shows that a reaction progress variable based on O_2 mass fraction can reliably be used in the characterisation of an EGR-type MILD combustion process for both methane and n-heptane. Furthermore, the reaction rate of the O_2 mass fraction-based reaction progress variable exhibits a strong positive correlation with the heat release rate for both methane and n-heptane MILD combustion. However, the interdependence of reactive scalars in the EGR-type homogeneous mixture combustion is found to be considerably different from that in the corresponding 1D unstretched laminar premixed flame. This indicates that a tabulated chemistry approach based on premixed laminar flames may not be valid under MILD conditions.

It is worth noting that linear combination of different species mass fractions (e.g. CO, CO_2, H_2 and H_2O) (Ihme and See 2011; Göktolga et al. 2017; Romero-Anton et al. 2020) can also be used to define the reaction progress variable. It has been found that this reaction progress variable is strongly positively correlated with O_2 mass fraction-based reaction progress variable with a roughly linear dependence between each other for both methane and n-heptane cases. However, the reaction progress variable definition based on a linear combination of mass fractions of different species, despite yielding an improved correlation between the reaction rate and heat release rate, gives rise to additional complexities in terms of the specification of the reaction progress variable diffusivity. The treatment of the diffusivity for a reaction progress variable based on a linear combination of different species mass fractions is not a straightforward task and might be strongly dependent on the choice of transport mechanism (de Swart et al. 2010; Abtahizadeh et al. 2015). The reaction rates and scalar dissipation rates and their interdependence for both O_2 mass fraction-based reaction progress variable and the reaction progress variable based on a linear combination of CO, CO_2, H_2 and H_2O mass fractions show qualitatively similar behaviours. The above information on the behaviour of the normalised mass fraction variations of individual major species provides the basis for future investigations involving automated methodologies for the definition of reaction progress variable, which is kept beyond the scope of the current work. Furthermore, the heat release rate and reaction rate of these reaction progress variables are found to be non-linearly related to the SDR of the reaction progress variable for both methane and n-heptane cases, but the qualitative behaviour is significantly different for these two fuels. This suggests that the range of the validity of the SDR-based reaction rate closure can be different for MILD combustion of different fuels.

It is important to note that a single reaction progress variable on its own might not be sufficient to characterise the reaction states in MILD combustion even for homogeneous mixtures

(where the equivalence ratio does not change). For example, the temperature should be accounted for separately in homogeneous mixture MILD combustion and a reaction progress variable based on temperature may not be able to describe the reaction state of the combustion process under MILD conditions. Thus, the present analysis only assesses the relative merits of different reaction progress variable definitions based on a-priori DNS analysis which is a well-established approach (e.g. Minamoto and Swaminathan 2015) to assess modelling hypotheses independent of other aspects. However, the practical implications of the relative merits of the usage of the reaction progress variable definition based on O_2 mass fraction and the linear combination of CO, CO_2, H_2 and H_2O mass fractions in actual RANS/LES simulations need to be investigated. The outcome of a RANS/LES simulation in terms of the comparison of its results with DNS/experimental data depends not only on the choice of the reaction progress variable but also on the closures of sub-grid stresses, sub-grid fluxes and the filtered reaction rate closure. Moreover, the modelling errors arising from these effects also interact with the numerical errors. Thus, the effects of the choice of the reaction progress variable cannot be ascertained straightforwardly based on RANS/LES simulations and this aspect is beyond the scope of the current analysis but will form the basis of future analyses.

Appendix A

Figure 7 shows a comparison between the non-dimensional temperature, reaction progress variables based on fuel, CO_2, and H_2O as functions of c_{O2} calculated from both a 1D diluted laminar premixed flame and 0D homogeneous constant pressure, ideal gas reactor with the initial states in Table 2. It can be seen from Fig. 7 that, for both configurations, the reactions progress variables and non-dimensional temperature have qualitatively similar profiles.

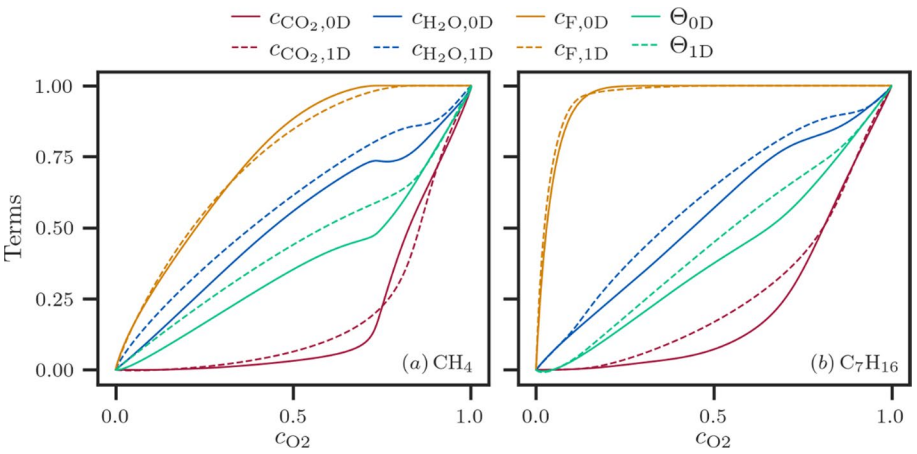

Fig. 7 Profiles of c_F, c_{CO2}, c_{H2O} and Θ conditional upon c_{O2} and calculated from 1D diluted laminar premixed flame as well as 0D homogeneous constant pressure reactor for CH_4 (**a**) and C_7H_{16} (**b**) cases

Appendix B

The behaviour of the non-dimensional temperature Θ in the turbulent MILD cases could benefit from an additional elucidation. It remains infeasible to categorically isolate a single reason for the behaviour of the non-dimensional temperature (Θ) in the turbulent cases (shown in Fig. 2). However, to illustrate the local distribution of Θ in the turbulent cases in the region $c_{O2} \gtrsim 0.9$ ($c_c \gtrsim 0.9$), the scatter of Θ with c_{O2} and c_c are shown in Fig. 8.

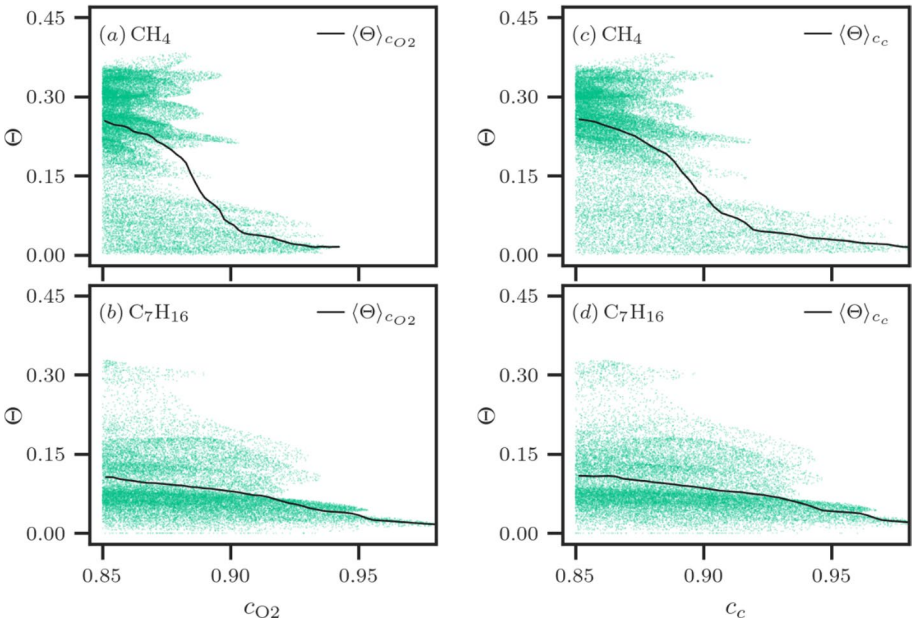

Fig. 8 Variation of the mean values of Θ conditioned upon c_{O2} and c_c in the regions $c_{O2} \gtrsim 0.9$ and $c_c \gtrsim 0.9$, respectively, along with instantaneous Θ scatter for CH_4 (**a, c**) and C_7H_{16} (**b, d**)

Acknowledgements The authors are grateful to EPSRC (EP/S025154/1 & EP/S025650/1) and ARCHER2 (EP/R029369/1) for the financial and computational support, respectively.

Author Contributions NC, KA and NS conceptualised the analysis. KA and NC conceptualised the simulations. HA and KA performed the simulations. HA and KA conducted the analysis. KA prepared the figures. NC wrote the original draft of the paper. NC, KA and UA supervised HA. NC and NS acquired the funding. KA, NC and NS reviewed and revised the manuscript.

Declarations

Conflict of interest The authors do not have any competing interests to declare that are relevant to the content of this article.

Ethics Approval This study does not involve any research with human participants and/or animals, so no ethical approval was required.

Informed Consent This study does not involve any research with human participants animals, so no informed consent was required.

References

Abo-Amsha, K., Chakraborty, N.: Surface density function and its evolution in homogeneous and inhomogeneous mixture *n*-heptane MILD combustion. Combust. Sci. Technol. (2023). https://doi.org/10.1080/00102202.2023.2182197

Abtahizadeh, E., de Goey, L.P.H., van Oijen, J.A.: Development of a novel flamelet-based model to include preferential diffusion effects in autoignition of CH4/H2 flames. Combust. Flame **162**, 4358–4369 (2015)

Aminian, J., Galletti, C., Shahhosseini, S., Tognotti, L.: Key modeling issues in prediction of minor species in diluted-preheated combustion conditions. Appl. Therm. Eng. **31**, 3287–3300 (2011)

Aminian, J., Galletti, C., Shahhosseini, S., Tognotti, L.: Numerical investigation of a MILD combustion burner: analysis of mixing field, chemical kinetics and turbulence-chemistry interaction. Flow Turb. Combust. **88**, 597–623 (2012)

Awad, H.S.A.M., Abo-Amsha, K., Ahmed, U., Chakraborty, N.: Comparison of the reactive scalar gradient evolution between homogeneous MILD combustion and premixed turbulent flames. Energies **14**, 7677 (2021)

Awad, H.S., Abo-Amsha, K., Ahmed, U., Klein, M., Chakraborty, N.: Assessment of Damköhler's hypotheses in the thin reaction zones regime using multi-step chemistry Direct Numerical Simulations of statistically planar turbulent premixed flames. Phys. Fluids **34**, 055120 (2022)

Awad, H.S.A.M., Abo-Amsha, K., Ahmed, U., Chakraborty, N.: A priori Direct Numerical Simulation assessment of MILD combustion modelling in the context of Reynolds Averaged Navier–Stokes Simulations, Flow. Turb. Combust. **111**, 799–823 (2023)

Bray, K.N.C.: Turbulent flows with premixed reactants. In: Libby, P.A., Williams, F.A. (eds.) Turbulent Reacting Flows, pp. 115–183. Springer, Berlin (1980)

Byrne, G.D.: Pragmatic experiments with Krylov methods in the stiff ODE setting. In: Cash, J., Gladwell, I. (eds.) Computational Ordinary Preferential Equations, pp. 323–356. Oxford University Press, Oxford (1992)

Cant, R.S.: Technical Report CUED/A-THERMO/TR67. Cambridge University Engineering Department, Cambridge (2012)

Cavaliere, A., de Joannon, M.: Mild combustion. Prog. Energy Combust. Sci. **30**, 329–366 (2004)

Chakraborty, N., Champion, M., Mura, A., Swaminathan, N.: Scalar dissipation rate approach to reaction rate closure. In: Swaminathan, N., Bray, K.N.C. (eds.) Turbulent premixed flame, 1st edn., pp. 74–102. Cambridge University Press, Cambridge (2011)

Chen, Z., Reddy, V.M., Ruan, S., Doan, N.A.K., Roberts, W.L., Swaminathan, N.: Simulation of MILD combustion using Perfectly Stirred Reactor model. Proc. Combust. Inst. **36**, 4279–4286 (2017)

Christo, F.C., Dally, B.B.: Modeling turbulent reacting jets issuing into a hot and diluted coflow. Combust. Flame **142**, 117–129 (2005)

Coelho, P.J., Peters, N.: Numerical simulation of a mild combustion burner. Combust. Flame **124**, 503–518 (2001)

Dally, B.B., Karpetis, A.N., Barlow, R.S.: Structure of turbulent non-premixed jet flames in a diluted hot coflow. Proc. Combust. Inst. **29**, 1147–1154 (2002)

Dally, B.B., Riesmeier, E., Peters, N.: Effect of fuel mixture on moderate and intense low oxygen dilution combustion. Combust. Flame **137**, 418–431 (2004)

De, A., Dongre, A.: Assessment of turbulence-chemistry interaction models in MILD combustion regime. Flow Turb. Combust. **94**, 439–478 (2015)

de Swart, J.A.M., Bastiaans, R.J.M., van Oijen, J.A., de Goey, L.P.H., Cant, R.S.: Inclusion of preferential diffusion in simulations of premixed combustion of hydrogen/methane mixtures with flamelet generated manifolds. Flow Turb. Combust. **85**, 473–511 (2010)

Dinkelacker, F., Manickam, B., Muppala, S.P.R.: Modelling and simulation of lean premixed turbulent methane/hydrogen/air flames with an effective Lewis number approach. Combust. Flame **158**, 1742–1749 (2011)
Doan, N.A.K., Swaminathan, N., Minamoto, Y.: DNS of MILD combustion with mixture fraction variations. Combust. Flame **189**, 173–189 (2018)
Duwig, C., Stankovic, D., Fuchs, L., Li, G., Gutmark, E.: Experimental and numerical study of flameless combustion in a model gas turbine combustor. Combust. Sci. Technol. **180**, 279–295 (2007)
Duwig, C., Stankovic, D., Fuchs, L., Li, G.: Experimental and numerical study of flameless combustion in a model gas turbine combustor. Combust. Sci. Technol. **180**, 279–295 (2008)
Duwig, C., Li, B., Li, Z.S., Aldén, M.: High resolution imaging of flameless and distributed turbulent combustion. Combust. Flame **159**, 306–316 (2012)
Eswaran, V., Pope, S.B.: Direct numerical simulations of the turbulent mixing of a passive scalar. Phys. Fluids **31**, 506–520 (1988)
Göktolga, M.U., van Oijen, J.A., de Goey, L.P.H.: Modeling MILD combustion using a novel multistage FGM method. Proc. Combust. Inst. **36**, 4269–4277 (2017)
Hadadpour, A., Xu, S., Zhang, Y., Bai, X.-S., Jangi, M.: An extended FGM model with transported PDF for LES of spray combustion. Proc. Combust. Inst. **39**, 4889–4898 (2023)
Huang, X., Tummers, M.J., van Veen, E.H., Roekaerts, D.: Modelling of MILD combustion in a lab-scale furnace with an extended FGM model including turbulence–radiation interaction. Combust. Flame **237**, 111634 (2022)
Ihme, M., See, Y.C.: LES flamelet modeling of a three-stream MILD combustor: analysis of flame sensitivity to scalar inflow conditions. Proc. Combust. Inst. **33**, 1309–1317 (2011)
Ihme, M., Shunn, L., Zhang, J.: Regularization of reaction progress variable for application to flamelet-based combustion models. J. Comput. Phys. **231**, 7715–7721 (2012)
Keil, F.B., Amzehnhoff, M., Ahmed, U., Chakraborty, N., Klein, M.: Comparison of flame propagation statistics extracted from DNS based on simple and detailed chemistry Part 2: influence of choice of reaction progress variable. Energies **14**, 5695 (2021)
Lamouroux, J., Ihme, M., Fiorina, B., Gicquel, O.: Tabulated chemistry approach for diluted combustion regimes with internal recirculation and heat losses. Combust. Flame **161**, 2120–2136 (2014)
Langella, I., Swaminathan, N., Pitz, R.: Application of unstrained flamelet SGS closure for multi-regime premixed combustion. Combust. Flame **173**, 161–178 (2016)
Liu, S., Hewson, J.C., Chen, J.H., Pitsch, H.: Effects of strain rate on high-pressure nonpremixed n-heptane autoignition in counterflow. Combust. Flame **137**, 320–339 (2004)
Medwell, P.R., Kalt, P.A., Dally, B.B.: Simultaneous imaging of OH, formaldehyde, and temperature of turbulent nonpremixed jet flames in a heated and diluted coflow. Combust. Flame **148**, 48–61 (2007)
Minamoto, Y., Swaminathan, N.: Scalar gradient behaviour in MILD combustion. Combust. Flame **161**, 1063–1075 (2014a)
Minamoto, Y., Swaminathan, N.: Modelling paradigms for MILD combustion. Int. J. Eng. Sci. Appl. Math. **6**, 65–75 (2014b)
Minamoto, Y., Swaminathan, N.: Subgrid scale modelling for MILD combustion. Proc. Combust. Inst. **35**, 3529–3536 (2015)
Minamoto, Y., Dunstan, T.D., Swaminathan, N., Cant, R.S.: DNS of EGR-type turbulent flame in MILD condition. Proc. Combust. Inst. **34**, 3231–3238 (2013)
Minamoto, Y., Swaminathan, N., Cant, R.S., Leung, T.: Morphological and statistical features of reaction zones in MILD and premixed combustion. Combust. Flame **161**, 2801–2814 (2014)
Najafi-Yazdi, A., Cuenot, B., Mongeau, L.: Systematic definition of progress variables and Intrinsically Low-Dimensional, Flamelet Generated Manifolds for chemistry tabulation. Combust. Flame **159**, 1197–1204 (2012)
Nguyen, P.-D., Vervisch, L., Subramanian, V., Domingo, P.: Multidimensional flamelet-generated manifolds for partially premixed combustion. Combust. Flame **157**, 43–61 (2010)
Niu, Y.-S., Vervisch, L., Tao, P.D.: An optimization-based approach to detailed chemistry tabulation: automated progress variable definition. Combust. Flame **160**, 776–785 (2013)
Oldenhof, E., Tummers, M.J., van Veen, E.H., Roekaerts, D.J.E.M.: Role of entrainment in the stabilisation of jet-in-hot-coflow flames. Combust. Flame **158**, 1553–1563 (2011)
Özdemir, I.B., Peters, N.: Characteristics of the reaction zone in a combustor operating at mild combustion. Expt. Fluids **30**, 683–695 (2001)
Papapostolou, V., Chakraborty, N., Klein, M., Im, H.G.: Effects of reaction progress variable definition on the Flame Surface Density transport statistics and closure for different combustion regime. Combust. Sci. Technol. **191**, 1276–1293 (2019)

Plessing, T., Peters, N., Wünning, J.G.: Laser optical investigation of highly preheated combustion with strong exhaust gas recirculation. Proc. Combust. Inst. **27**, 3197–3204 (1998)
Poinsot, T., Veynante, D.: Theoretical and Numerical Combustion. R.T. Edwards Inc., Philadelphia (2001)
Proch, F., Domingo, P., Vervisch, L., Kempf, A.M.: Flame resolved simulation of a turbulent premixed bluff-body burner experiment. Part I: Analysis of the reaction zone dynamics with tabulated chemistry. Combust. Flame **181**, 321–339 (2017)
Prüfert, U., Hartl, S., Hunger, F., Messig, D., Eiermann, M., Hasse, C.: A constrained control approach for the automated choice of an optimal progress variable for chemistry tabulation. Flow Turb. Combust. **94**, 593–617 (2015)
Rahnama, P., Maghbouli, A., Bao, H., Vasavan, A., Novella, R., Somers, B.: Generalizing progress variable definition in CFD simulation of combustion systems using tabulated chemistry models. Appl. Energy Combust. Sci **14**, 100132 (2023)
Rogallo, R.S.: Numerical experiments in homogeneous turbulence, NASA Technical Memorandum 81315, NASA Ames Research Center, California (1981).
Romero-Anton, N., Huang, X., Bao, H., Martin-Eskudero, K., Salazar-Herran, E., Roekaerts, D.: New extended eddy dissipation concept model for flameless combustion in furnaces. Combust. Flame **220**, 49–62 (2020)
Sidey, J., Mastorakos, E., Gordon, R.L.: Simulations of autoignition and laminar premixed flames in methane/air mixtures diluted with hot products. Combust. Sci. Technol. **186**, 453–465 (2014)
Smooke, M.D., Giovangigli, V.: Premixed and nonpremixed test flame results. Reduced kinetic mechanisms and asymptotic approximations for methane-air flames. Springer, pp. 29–47 (1991).
Sorrentino, G., Göktolga, U., de Joannon, M., van Oijen, J.A., Cavaliere, A., de Goey, P.: An experimental and numerical study of MILD combustion in a Cyclonic burner. Energy Procedia **120**, 649–656 (2017)
Suzukawa, Y., Sugiyama, S., Hino, Y., Ishioka, M., Mori, I.: Heat transfer improvement and Nox reduction by highly preheated air combustion. Energy Convers. Manag. **38**, 1061–1071 (1997)
Swaminathan, N.: Physical insights on MILD combustion from DNS. Front. Mech. Eng. **5**, 549 (2019)
Tsuji, O.H., Gupta, A.K., Hasegawa, T., Katsuki, M.: High Temperature Air Combustion: From Energy Conservation to Pollution Reduction. CRC Press, Boca Raton (2003)
van Oijen, J.A.: Direct numerical simulation of autoigniting mixing layers in MILD combustion. Proc. Combust. Inst. **34**, 1163–1171 (2013)
Vasavan, A., de Goey, P., van Oijen, J.: A novel method to automate FGM progress variable with application to igniting combustion systems. Combust. Theor. Modell. **24**, 221–244 (2020)
Ye, J., Medwell, P., Evans, M., Dally, B.: Characteristics of turbulent n-heptane jet flames in a hot and diluted coflow. Combust. Flame **183**, 330–342 (2017)